J. Phys. B: At. Mol. Opt. Phys. 24 (1991) 2579-2588. Printed in the UK

Abnormal behaviour of zero degree δ-electron emission on the projectile ionic charge*

O Jagutzki†, S Hagmann‡, H Schmidt-Böcking†, R E Olson§, D R Schultz§, R Dörner†, R Koch†, A Skutlartz||, A González¶°, T B Quinteros‡#, C Kelbch† and P Richard‡

† Institut für Kernphysik, Universität Frankfurt, D-6000 Frankfurt/M. 90, Federal Republic of Germany
‡ JR Macdonald Laboratory, Kansas State University, Manhattan KS 66506, USA
§ Physics Department, University of Missouri-Rolla, Rolla MO 65401, USA
|| Department of Physics, East Carolina State University, Greenville NC 27858, USA
¶ CONICET, Buenos Aires, Republica Argentina
# Present address: Manne Siegbahninstitutet för Fysik, S-10405 Stockholm, Sweden

Received 27 December 1990, in final form 13 March 1991

Abstract. The 0° δ-electron emission was investigated by an electron-projectile coincidence technique as a function of incoming and outgoing projectile charge state for 0.53 MeV u^{-1} Cu^{q+} on He. The electron emission spectra vary strongly with initial and final projectile charge state. For pure ionization channels the cross sections follow for low electron energy the q^2-scaling law whereas in the binary encounter regime the scaling is reversed. CTMC calculations are in fair agreement with the experimental data.

1. Introduction

Recent experimental and theoretical studies of electron emission in fast partially stripped heavy ion-atom collisions revealed rather unexpected results. Kelbch *et al* (1989a, b) found for U^{33+} on rare gases surprising structures in the δ-electron spectrum for certain emission angles ϑ_e depending on the impact energy. Very recently Reinhold *et al* (1990, 1991) performed theoretical studies on the scattering of target electrons by a screened potential and could nicely reproduce these experimental data. The origin of these structures were attributed to rainbow- and glory-like scattering of electrons by the non-Coulomb potential of the incident screened ion. The structures in the angular and energy emission pattern of δ-electrons appear only for the impact of very heavy ions. However the influence of a screened potential is also visible for comparatively light ions.

Richard *et al* (1990) examined the binary encounter (BE) production cross section at $\vartheta_e = 0°$ for 1-2 MeV u^{-1} F^{q+} on H_2. They observed an increase of the BE cross section with decreasing projectile charge. This was in contradiction to the expectations (Gryzinski 1987, Toburen *et al* 1981, Stolterfoht 1978) and to the results of Lee *et al* (1990). They found for bare F, O, N, C ions colliding with H_2 and He an excellent

---

* Supported by DFG, BMFT and DOE.

° Present address: Det Fysiske Institut, Aarhus Universitet, DK-8000 Aarhus, Denmark.

0953-4075/91/102579+10$03.50

agreement with the q^2-scaling law derived from first-order perturbation theory, i.e. the BE cross section increases with increasing (bare) projectile charge.

Reinhold *et al* (1990) could nicely reproduce the experimental data of Richard *et al* (1990) extending the classical BE approximation (Gryzinski 1987) for partially stripped ions. Based on the CTMC model Olson *et al* (1990) calculated δ-electron emission cross sections differential in energy and emission angle for heavy ion impact on Ar showing that a screened projectile potential can significantly enhance the cross sections for BE electron emission in the forward direction ($\vartheta_e \leqslant 20°$).

In order to understand the mechanism of how the screening of the projectile charge can influence so dramatically the emission of highly energetic electrons in fast ion–atom collisions it is important to determine the final charge state of the projectile. Thus one can determine, for instance, whether a significant contribution to the enhanced cross sections results from the ionization of projectile electrons (electron loss).

Quinteros *et al* (1991) demonstrated by means of an electron–projectile coincidence technique that the influence of projectile loss or capture channels on the total 0° BE cross section in 0.53 MeV u^{-1} F^{q+} on H_2 is almost negligible. The unexpected scaling of the BE cross section with the initial charge state (Richard *et al* 1990) is also observed with good quantitative agreement in the pure ionization channel, i.e. when no projectile charge change occurs.

Furthermore, the results summarized above might be very important for radiation research since for kinematic reasons especially the forward δ-electrons gain higher kinetic energies and thus contribute more to radiation damage. In contradiction to the expectations this means that a projectile with low (screened) charge may produce more 'hot' electrons than the corresponding bare ion.

Since coincidence measurements with well defined incoming (q_i) and outgoing (q_f) projectile charge states seem to be an appropriate method to reveal further details of the δ-electron emission features in collisions with partially stripped ions we have performed an electron-projectile coincidence for the collision system 0.53 MeV u^{-1} Cu^{q+} on He. The electron spectra have been measured for different $q_i - q_f$ reactions.

CTMC (classical trajectory Monte Carlo) calculations also differential in q_f have been performed to accomplish our considerations. The method has been described previously in Olson *et al* (1990). The screening effect of the projectile electrons was approximated by the choice of a static non-Coulomb potential for partially stripped ions.

We have found for low energy electrons (soft collisions) a scaling of the cross section with q_i^2. This is in agreement with the expectations since for these collisions at large distances the electrons sense a point-like $1/r$ potential. Instead, for higher δ-electron energies we find a strong deviation from the q_i^2 dependence. In the BE regime the q_i^2 scaling is even reversed.

2. Experiment

The experiment has been performed at the 6 MV EN Tandem accelerator of the JR Macdonald Laboratory at Kansas State University. Figure 1 shows a schematic sketch of the experimental set-up. The set-up is similar to the one described by Quinteros *et al* (1991). The beams of 0.53 MeV u^{-1} Cu^{5+} and Cu^{15+} were tightly collimated over 7 m collimation length with three adjustable four-jaw slit systems. The target was

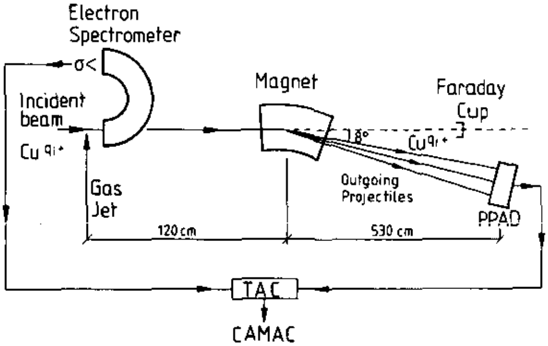

Figure 1. Sketch of the experimental set-up.

formed by a hypodermic needle effusing He into the interaction region. The gas target pressure was kept constant within 5%. Single collision conditions have been verified experimentally. The beamline vacuum conditions were better than 5×10^{-7} Torr.

Electrons ejected from the target at $\vartheta_e = 0°$ into a solid angle of 1.8×10^{-2} sr were energy analysed by an electrostatic hemispherical electron analyser and then detected using a channel electron multiplier. The voltage was scanned with low repetition rate to monitor electron spectra between 70 and 2000 eV with an energy resolution of 1.5%. A double μ-metal shielding surrounded the target region. Thus the electron spectra were not affected by magnetic fields. Figure 2 shows an electron spectrum for 0.53 MeV u^{-1} Cu^{15+} on He.

The projectiles were magnetically charge state analysed 1.2 m downstream from the target and then detected using a parallel-plate avalanche detector (PPAD) with a stripe anode position sensitive in one dimension (Gaukler *et al* 1977). Thus different outgoing projectile charge states could be detected simultaneously. The detection efficiency for each stripe has been checked carefully. It approaches practically 100%.

The coincident events were determined by a standard fast-slow coincidence technique and recorded in list mode using a CAMAC/μ-VAX data acquisition system. The TAC was started by electrons and stopped by the charge state analysed projectiles.

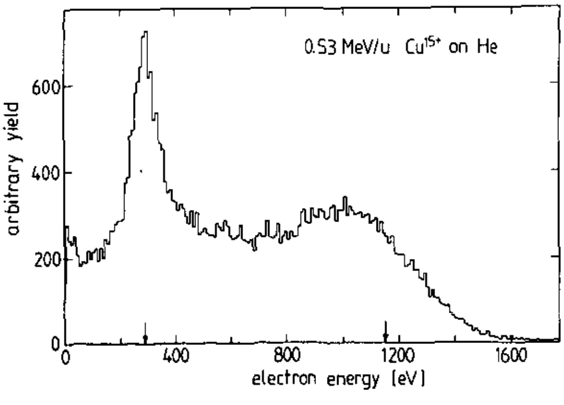

Figure 2. 0° electron spectrum for 0.53 MeV u^{-1} Cu^{15+} on He. The spectrum is not corrected for the spectrometer transmission function (proportional to $1/E$). The arrows mark the position of the cusp and BE peak (classically calculated).

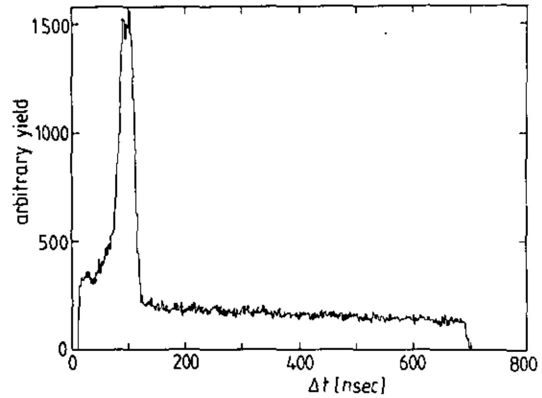

Figure 3. Time spectrum for $q_i = q_f = 15+$. The spectrum is summed over all electron energies (different flight times) so that the apparent width of the time peak is broader than the time resolution of about 17 ns.

Figure 3 shows a typical time spectrum. The time resolution was about 17 ns. The coincident electron spectra were corrected for random events and contributions of beam impurities.

The double differential cross section for the δ-electron emission at $\vartheta_e = 0°$ is given by

$$\frac{\Delta^2}{\Delta E_e \Delta\Omega_e}(q_i, q_f) = \frac{N_e(\Delta E_e, q_i, q_f)}{N_{tot}(q_i)}\, c. \tag{1}$$

$N_e(\Delta E_e, q_i, q_f)$ is the number of true events in the electron energy window ΔE_e coincident with projectiles of initial (i) and final (f) charge state q_i and q_f. $N_{tot}(q_i)$ is the total number of incoming projectiles with charge state q_i

$$N_{tot}(q_i) = \sum_f N_P(q_i, q_f) \tag{2}$$

$N_P(q_i, q_f)$ is the number of detected particles of initial and final charge states q_i and q_f. The constant c is independent of q_f and contains the spectrometer transmission, the electron detection efficiency and the target density. Since c is only roughly known for our set-up the experimentally determined cross sections are only relative. Nevertheless, a comparison between different (q_i, q_f) reaction channels is possible because c was kept constant for all our measurements.

The error bars in the figures are due to statistics and for $q_i \neq q_f$ also to uncertainties in the determination of beam contaminations.

3. Results and discussion

In figure 4 the measured 0° δ-electron cross sections $\Delta^2\sigma/\Delta E \Delta\Omega\ (q_i, q_f = q_i)$ for $q_i = 5+$ and 15+ are presented. A significantly different shape is immediately obvious. The BE peak is more pronounced for $q_i = 5+$. For low electron energies the $q_i = 15+$ spectrum exceeds the $q_i = 5+$ curve but shows in the BE region only a shoulder and the more energetic δ electrons are strongly reduced compared with the Cu^{5+} spectrum.

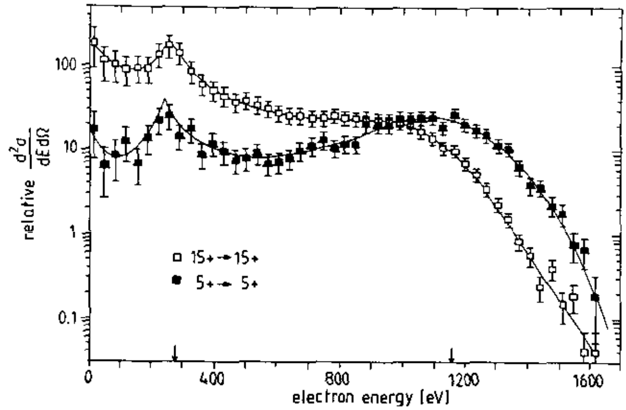

Figure 4. Measured relative δ-electron emission cross sections for $q_i = q_f = 5+$, 15+ (pure ionization channels). The curves are drawn to guide the eye.

Considering the ratio of the cross section for $q_i = 5+$ and 15+ (figure 5) a dramatic q-scaling variation with the electron energy is obvious. The q^2 scaling indicated by the chain line is valid only for ionized electrons on the low-energy side of the cusp peak. This is expected since these δ electrons originate from soft collisions at large projectile-electron impact parameters, i.e. where the screened projectile potential follows q_i/r.

We assume that for increasing δ-electron energy the collisions get closer on average, because large momentum transfers require strong Coulomb forces, i.e. small distances. Generally, a small nuclear impact parameter leads also to smaller projectile-electron impact parameters because the electron density peaks at the target nucleus. As the distance between projectile and target electrons becomes smaller, the electrons experience more and more the unscreened charge Z_P of the bare nucleus. For ionization reactions producing δ electrons at $\vartheta_e \approx 0°$ with a velocity of twice the projectile velocity, thus projectile-electron binary collisions with much smaller impact parameters are dominating. The electron feels the entire potential of the nucleus unscreened by the

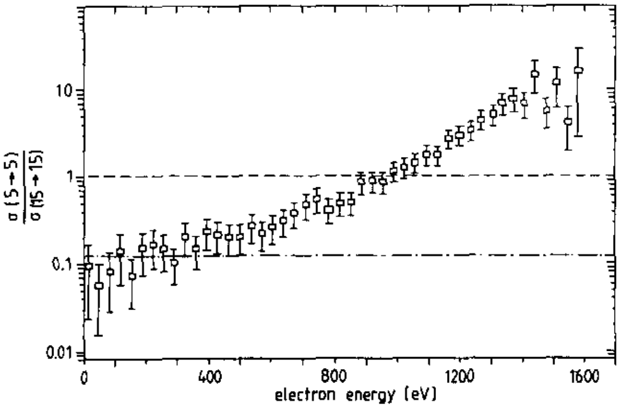

Figure 5. Ratio between the measured relative δ-electron emission cross sections of $q_i = q_f = 5+$ and $q_i = q_f = 15+$ (pure ionization channels). The broken line marks a Z_P^2 scaling, the chain line indicates a q_i^2 scaling.

remaining projectile electrons. In this BE regime the cross sections for different q_i should be equal and depend only on Z_P (indicated by the broken curve in figure 5). This scaling behaviour is indeed found for light ion impact (Reinhold and Schultz 1989).

For a heavy ion like Cu^{q+}, however, the q scaling beyond the BE energy is reversed. So our experiments demonstrate for the first time that partially stripped ions do not only have a higher production cross section for high energetic δ electrons than the corresponding highly stripped ion, but that the spectral shape deviates significantly and the emission of higher energy electrons ($E_\delta \gg E_{BE}$) in the forward direction is favoured for less stripped projectiles.

In figure 6 CTMC calculations of 0° electron emission cross sections for the pure ionization channels $q_i = q_f = 5+$, $15+$ and $29+$ are shown. Fair agreement with our data is observed. The theory predicts for $q_i = 29+$ (completely stripped) an even more dramatic supression of high energetic δ electrons. This unexpected behaviour might be explained qualitatively by the following mechanisms.

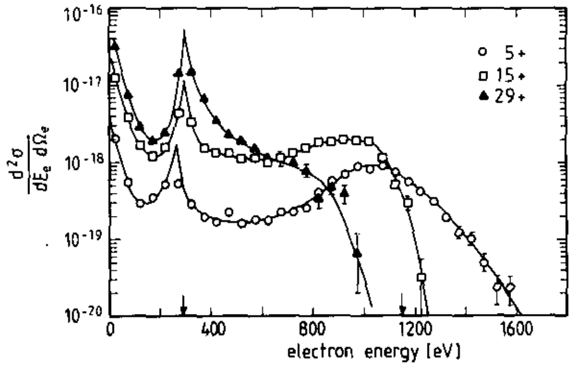

Figure 6. Absolute δ-electron emission cross sections in units of $cm^2\, eV^{-1}\, sr^{-1}$ for $q_i = q_f = 5+$, $15+$ and $29+$ (pure ionization channels) obtained by calculations based on the CTMC model. The curves are drawn to guide the eye.

(i) For the bare Cu^{29+} the capture cross section is huge. Especially at small impact parameters where the production of high energetic 0° δ electrons takes place, the probability for simultaneous capture is very high. Therefore the BE electrons should appear predominantly in the capture channel, i.e. with $q_f = 28+$.

(ii) A projectile with $q = 29+$ can effectively ionize the target atom already at large internuclear distances R. This 'soft' ionization leads to low-energy δ electrons mainly ejected at $\vartheta_e \approx 90°$. When the projectile finally advances to the distance of closest approach, where the high-energy forward directed electrons are produced, the target is already highly ionized or even bare in the case of light targets like He. Thus although the total ionization cross section (integrated over all electron energies and emission angles) scales with q^2, the cross section for high-energy forward electron emission ('hard' ionization) is strongly reduced and will therefore show an abnormal q dependence.

In this picture also the findings of Richard *et al* (1990), Reinhold *et al* (1990), Olson *et al* (1990) and Quínteros *et al* (1991) can be understood. An approaching projectile with charge q and nuclear charge Z_P screened by n core electrons ($n + q = Z_P$) might already ionize less target electrons at large internuclear distances R on the incoming part of the trajectory than the bare ion ($Z_P = q$). The target atom already reaches a higher ionization stage for large distances during the approach of a bare ion than for a stripped ion acting as a point charge of smaller magnitude $(Z_P - n)$. Later, when the projectile advances to the target nucleus (small R), the residual target electrons experience the unscreened field of the projectile nucleus which is the same for bare or partially stripped ion impact. The bare ion has removed already more electrons in early collision stages and the residual electrons are bound tighter, whereas the partially stripped ion still finds more remaining weakly bound target electrons that can be ionized via a 'hard' binary collision. The screening of the projectile nucleus charge prevents an early ionization of the target atom, i.e. keeps it in a low ionization stage before the entire projectile nucleus charge is uncovered at small distances. Thus, due to the lower target ionization prior in the collision the partially stripped ion will produce more high energetic 0° BE electrons.

This picture of the partially stripped ion acting as a 'wolf in a sheep's clothing' is very intuitive but of course cannot serve as a basis for detailed quantitative investigations. Especially, the influence of the projectile charge on possible polarization effects is neglected.

In order to determine the influence of projectile electron loss and capture of target electrons into the projectile bound states we measured these reaction channels too. In figures 7 and 8 the relative double differential cross sections of the pure ionization channel compared with channels where simultaneously a loss or capture occurs are displayed. For $q_i = 15+$ (figure 7) capture and loss channels contribute only a few per cent to the total δ-electron specta summed over all q_f. We can therefore conclude that the suppression of highly energetic δ electrons in the 0° ionization spectrum for $q_i = q_f = 15+$ is not due to the fact that these electrons are predominantly emitted with simultaneous projectile charge change channels; i.e. the highly energetic δ electrons do not appear in other reaction channels as might be the case for $q_i = q_f = 29+$ (mechanism (i), see above).

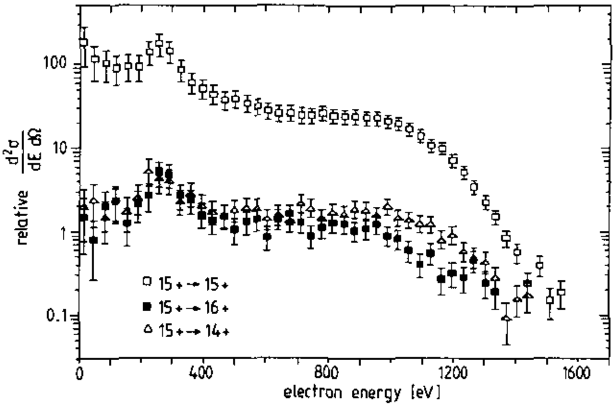

Figure 7. Measured relative δ-electron emission cross sections for incoming Cu^{15+} ions coincident with different outgoing projectile charge states.

For $q_i = 5+$ (figure 8), however, the loss channel contributes strongly to the electron yield integrated over all q_f. Adding the loss contribution to the pure ionization channel one finds that for $q_i = 5+$ even more highly energetic 0° δ electrons are produced than expected from figures 4 and 5. The capture channel ($q_i = 5+$, $q_f = 4+$) was found to

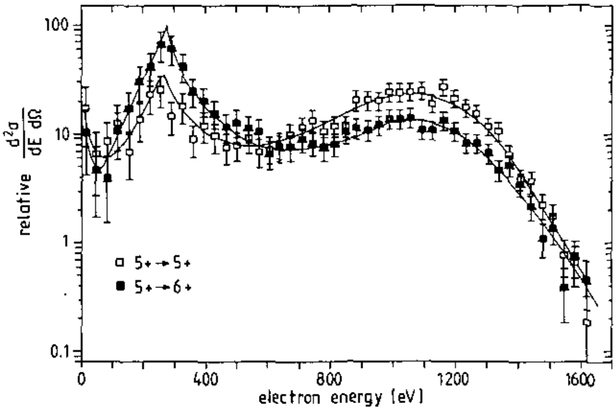

Figure 8. Measured relative δ-relative emission cross sections of pure ionization ($q_f = 5+$) and loss channel ($q_f = 6+$) for incoming Cu^{5+}. The lines are drawn to guide the eye.

give a contribution below 1% and was therefore not investigated in detail. Thus we conclude that the ratio of the ionization cross sections shown in figure 5 is really due to the particular scattering features of target electrons in the screened projectile potential.

To discuss the loss and capture channels in a little more detail ratios of double differential cross sections for channels with charge exchange and the pure ionization are presented in figures 9 and 10. For $q_i = 15+$ the ratio both for capture and loss increases towards higher electron energies. This can be explained qualitatively in the impact parameter picture (Quinteros *et al* 1990). It is well known that capture and loss reactions are occurring predominantly at smaller impact parameters compared with pure ionization. Since CTMC calculations predict that high energetic electrons are

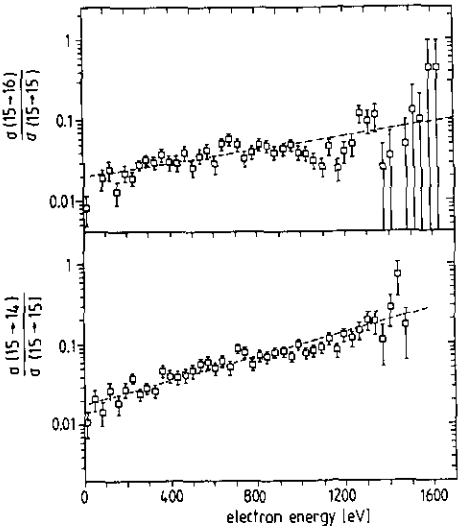

Figure 9. Ratio of measured δ-electron emission cross sections between the pure ionization channel and the loss and capture channels respectively for incoming Cu^{15+} projectiles. The lines are drawn to guide the eye.

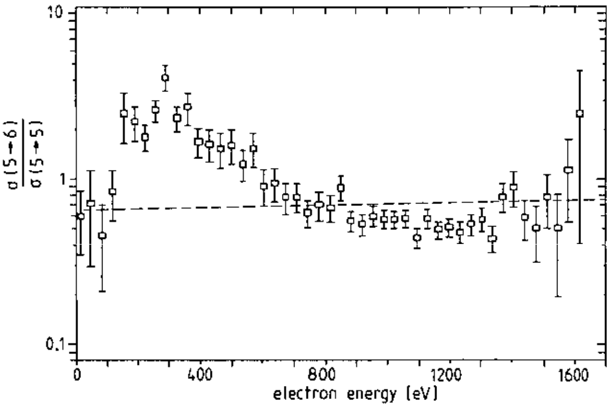

Figure 10. Ratio of the measured δ-electron emission cross sections between the pure ionization channel and the loss channel for incoming Cu^{5+} projectiles. The line qualitatively indicates the ratio expected without projectile loss electrons.

also produced with much higher probability in the small-b regime the detection of a loss or capture process favours the observation of an highly energetic δ electron compared with projectiles not charge exchanged. For low-energy electrons we expect in agreement with the data the opposite behaviour because these δ electrons result from soft collisions at large impact parameters.

For $q_i = 5+$ the cross section ratio between loss channel and pure ionization shows a strong enhancement around the cusp energy. This is due to the huge cross section of Cu^{5+} for electron loss to the continuum (ELC). Projectile electrons are scattered into low-lying projectile continuum states. This mechanism can only appear in loss channels (one projectile electron is stripped off). Since the electrons in Cu^{15+} are tightly bound, ELC is of minor importance there. Beyond the ELC regime the energy dependence of the ratio in figure 10 is in agreement with our picture described above for $q_i = 15+$.

The fact that the cross sections for 'hot' electrons produced by partially stripped heavy ions impinging on atoms do not at all scale with q^2 has consequences for the field of radiation damage by heavy ion impact. It is assumed that the radiation damage is proportional to the electronic stopping cross section $S = \int E_e \sigma(E_e, \vartheta_e)\, dE_e\, d\vartheta_e$ integrated over all electron energies E_e and emission angles ϑ_e, i.e. the ionization cross section is weighted with the corresponding electron energy. Using our experimental data we find for the cross sections for $\vartheta_e = 0°$ integrated over the investigated energy range and summed over all detected (i.e. significantly contributing) q_f that $\sigma(q_i = 15+, \vartheta_e = 0°)$ and $\sigma(q_i = 5+, \vartheta_e = 0°)$ are almost equal. Defining $S_0 = S(\vartheta_e = 0°)$ one finds that $S_0(q_i = 5+)$ exceeds $S_0(q_f = 15+)$ by a factor of 1.4. This means that for ions penetrating matter the stopping cross section of 'hot' ionized electrons emitted into the inner core of the ionic track does not at all scale with q^2. On the contrary, less stripped (i.e. less charged) ions may contribute more to radiation damage since S_0 yields an important portion of the total S.

Although we have so far only considered collisions of fast ions with atomic targets, we assume that our findings are valid for solid targets too, since the binding properties of the target electrons seem not to affect the scattering features of the electrons on a screened potential in the high energy limit. It is to be noted, however, that for a detailed quantitative estimation a consideration of electron emission into the other ϑ_e is required including investigations with solid targets. Nevertheless, the data presented here indicate that the process of heavy-ion-induced radiation damage is much more complex than commonly expected.

4. Conclusion

Investigating the production of 0° δ electrons in collisions of fast heavy ions with He both experimentally and theoretically we found evidence that the screening of the projectile ionic charge strongly affects the differential cross section for high energetic electron emission. The common q^2-scaling law is dramatically violated. The CTMC theory reproduces the experimental data. The determination of the outgoing projectile charge state made it possible to exclude the influence of loss or capture channels. The results obtained here might have a strong implication on the analysis of radiation damage induced by heavy ions.

References

Gaukler G, Schmidt-Böcking H, Schuch R, Schule R, Specht H J and Tserruya I 1977 *Nucl. Instrum. Methods* **141** 115

Gryzinski M 1987 *J. Phys. B: At. Mol. Phys.* **20** 4741

Kelbch C, Hagmann S, Kelbch S, Mann R, Olson R E, Schmidt S and Schmidt-Böcking H 1989a *Phys. Lett.* **139A** 304

Kelbch C, Olson R E, Schmidt S, Hagmann S and Schmidt-Böcking H 1989b *J. Phys. B: At. Mol. Opt. Phys.* **22** 2171

Lee D H, Richard P, Zouros T J M, Sanders J M and Shinpaugh J L 1990 *Phys. Rev.* A **41** 4816

Olson R E, Reinhold C O and Schultz D R 1990 *J. Phys. B: At. Mol. Opt. Phys.* **23** L455

Quinteros T B, Gonzales A D, Jagutzki O, Skutlartz A, Lee D H, Hagmann S, Richard P, Kelbch C, Varghese S L and Schmidt-Böcking H 1991 *J. Phys. B: At. Mol. Opt. Phys.* **24** 1377

Reinhold C O and Schultz D R 1989 *J. Phys. B: At. Mol. Opt. Phys.* **22** L565

Reinhold C O, Schultz D R and Olson R E 1990 *J. Phys. B: At. Mol. Opt. Phys.* **23** L591

Reinhold C O, Schultz D R, Olson R E, Kelbch C, Koch R and Schmidt-Böcking H 1991 *Phys. Rev. Lett.* **66** 1842

Richard P, Lee D H, Zouros T J M, Sanders J M and Shinpaugh J L 1990 *J. Phys. B: At. Mol. Opt. Phys.* **23** L213

Stolterfoht N 1978 *Structure and Collisions of Ions and Atoms* ed I A Sellin (Berlin: Springer) p 155

Toburen L H, Stolterfoht N, Ziem P and Schneider D 1981 *Phys. Rev.* A **24** 1741